Upregulation of TASK-3 Underlies Retraction of Spontaneous Activity in the Developing Mouse Hindbrain

Kelly Duong

A dissertation submitted in partial fulfillment of the requirements for the degree of

Doctor of Philosophy

University of Washington

2018

Reading Committee:

Larry Zweifel, Chair

William Moody

Martha Bosma

Program Authorized to Offer Degree:

Neuroscience

University of Washington

Abstract

Upregulation of TASK-3 Underlies Retraction of Spontaneous Activity in the Developing Mouse Hindbrain

Kelly Duong

Chair of the Supervisory Committee:

Martha Bosma

Department of Biology

The cessation of spontaneous activity (SA) is an important characteristic of this immature form of cellular excitability. While we have extensively documented the precise timing and patterning of mouse hindbrain SA, the mechanism behind its termination remained a mystery. For my thesis project, I sought to elucidate the molecular mechanism behind hindbrain SA retraction and subsequent termination. I hypothesized that a class of background leak potassium channels, K2P channels, were upregulated in the same spatiotemporal manner as SA retraction, allowing for the hyperpolarization of resting membrane potential that leads to the silencing of cellular activity. By pharmacologically targeting the precise K2P channel I identified to be upregulated, TASK-3, I was able to reactivate cells that had already been silenced. Finally, I utilized open-source transcriptome data to explore plausible biological pathways that might be linked to hindbrain SA regulation.

ACKNOWLEDGEMENTS

First of all, I need to thank my PhD advisor, Dr. Marti Bosma. The graduate school years overlap with a lot of significant life events. Marti has been a supportive figure and mentor, intellectually and emotionally, through many of my highs and lows. I'm incredibly grateful to have her as an advisor and friend, and I'll always cherish our candid conversations about science, politics, family, and food. I also have to thank Marti for allowing me to explore career options outside of academia. I genuinely believe that my time spent practicing science outside of an academic setting has made me a better scientist and a better colleague. Thanks to the rest of the Bosma lab, notably Hiro Watari, who did so much of the pioneering work for this project. Hiro is one of the most thorough scientists I've ever met and I was lucky to be given the opportunity to build upon his work. Thank you to my committee members: Larry Zweifel, Bill Moody, and Jihong Bai; the Neuroscience department chairs: Jane Sullivan, David Perkel, Horacio de la Iglesia, and Paul Phillips.

Lastly, I would never accomplish anything significant without the unconditional love of my family. My parents, Ut Nguyen and Toan Duong, always believed in me even when I tried to argue that things are really bad, but sometimes it's nice to have superfans cheering you on. My husband and BFF, Mark Richardson—thank you for striking the perfect balance between lightheartedness and sincerity

INTRODUCTION

Spontaneous electrical activity (SA) that occurs before the development of sensory systems has been shown to be necessary for synaptogenesis, circuit refinement, neurotransmitter specification, ion channel expression (Clause et al., 2014; Moody & Bosma, 2005; Spitzer, 2012). SA has been observed in many different species and in many different parts of the nervous system for any given species. One feature that has been used to characterize each instance of SA is the period of development it is restricted to. This leads to the mysteries of initiation and termination, both of which has been shown to vary between brain region and species. A common property of SA initiation is hyperexcitability, though the mechanism underlying cellular hyperexcitability varies between systems. Some mechanisms that would lead to hyperexcitability include functional recurrent connectivity, excess innervation, Cl^- being excitable in early development, or overexpression of glutamate receptors. In the mouse hindbrain, cells express T-type calcium channels that generate a "window current" from the overlap of the channel's activation and inactivation curves while the cell is at its resting potential (Moody & Bosma, 2005). This "window current" is the trigger for hindbrain SA. While the cellular properties that contribute to the initiation of SA in the mouse hindbrain has been studied, the mechanism behind SA termination is still poorly understood. Our lab previously published that hindbrain SA termination was due to progressive hyperpolarization of the resting membrane potential (Watari, Tose, & Bosma, 2013). My thesis project identified TASK-3 as the molecular regulator behind the membrane hyperpolarization. By targeting this gene we believe to be a crucial component to laying the spatiotemporal properties of hindbrain SA, we hope to gain insight into the role of SA in hindbrain development.

Spontaneous activity in the developing mouse hindbrain

SA in the developing mouse hindbrain is a highly regulated process with precise spatiotemporal characteristics. Intracellular Ca^{2+} oscillations are only detectable in the hindbrain over 5 days of embryonic development, with progressive retraction of the area participating in SA. Mouse hindbrain SA originates in a group of rostral midline cells called the initiation zone. From there, calcium waves propagate laterally and caudally across gap-junction-coupled cells (Hunt, McCabe, & Bosma, 2005). Under calcium imaging, spontaneous events appear at embryonic day 9.5 (E9.5) along the hindbrain midline and organizes into widely spreading synchronized waves at E11.5-12.5 before retracting from the lateral and caudal edges at E13.5. By E15.5, cells that previously participated in a network of propagating electrical activity are now silent. By altering the ionic conductance of cells that participate in SA, we were able to extend the period of SA experienced by the mouse hindbrain.

Hindbrain Anatomy and Function

During vertebrate embryonic development, hindbrain segmentation is present in the form of branchial arches and rhombomeres. Branchial arches are precursors for many muscle groups, cranial nerves, and bone structures found in the head. In fish, the branchial arches are known as gill arches because they develop into structures that support the gills.

Branchial arch-derived tissues include the pharynx and larynx which are innervated by the ninth and tenth cranial nerves, controlling swallowing and vocalization. Hindbrain cranial nerves control several muscle groups of the head and face. Fifth cranial nerve controls jaw muscles. Emotional displays through facial expressions are controlled by seventh cranial nerve.

Cranial nerves control muscles of the tongue and lip which allows for spoken language. Of the 12 mammalian cranial nerves, 8 are found in the hindbrain (I and II are forebrain nerves, III and IV are midbrain nerves).

Hindbrain segmentation can be observed in early embryonic development as visible bulges known as rhombomeres along the anterior-posterior access. Adjacent pairs of rhombomeres give rise to nerve fibers that innervate all muscles derived from a single branchial arch (Krumlauf & Keynes, 1994). For example, the trigeminal nerve is found within rhombomeres 2 and 3 and innervates all muscles of the first branchial arch.

Rhombomeres are specified genetically by Hox genes whose protein product are transcription factors. The mammalian hindbrain is segmented into 7 rhombomeres, each expressing a unique combination of Hox transcription factors. Hox genes are well-conserved DNA sequences that set the body plan in all animals from fruit flies to humans. The body of a fruit fly and other insects can be divided into 8 segments along the anterior-posterior axis, each expressing 1 of 8 unique Hox genes. Unlike insect Hox genes, there is redundancy and a gradient to mammalian Hox gene expression so that ablation of a single Hox gene can have little consequence. However, the combination produces a unique code based on the gene expressed and level of expression.

K2P channels

Two-pore domain potassium channels are background "leak" channels because they are open at normal physiological voltages. There are two common naming conventions that are used interchangeable throughout this thesis. The Human Genome Organization (HUGO) has assigned

each gene the prefix *KCNK* followed by a different number sequentially given based on when each gene was discovered (*KCNK1* was the first gene discovered, then *KCNK2* and so on). However, there are gaps between the assignments, probably due to the realization that some novel discoveries were actually just duplicates of an already-known gene. The HUGO naming convention spans *KCNK1* to *KCNK18* although there are only 15 unique genes.

The other naming system divides the 15 members into 7 subfamilies based on structural and functional properties (Feliciangeli, Chatelain, Bichet, & Lesage, 2014). The names are acronyms featuring functional attributes of each subfamily followed by a number:

1) TWIK: tandem of P domains in a weak inwardly rectifying K+ channel

   TWIK-1 (*KCNK1*), TWIK-2 (*KCNK6*), TWIK-3 (*KCNK7*)

2) THIK: tandem pore domain halothane-inhibited K+ channel

   THIK-1 (*KCNK13*), THIK-2 (*KCNK12*)

3) TREK: TWIK-related K+ channel

   TREK-1 (*KCNK2*), TREK-2 (*KCNK10*)

4) TASK: TWIK-related acid-sensitive K+ channel

   TASK-1 (*KCNK3*), TASK-2 (*KCNK5*), TASK-3 (*KCNK9*), TASK-5 (*KCNK15*)

5) TALK: TWIK-related alkaline pH activated K+ channel

   TALK-1 (*KCNK16*), TALK-2 (*KCNK17*)

6) TRESK: TWIK-related spinal cord K+ channel

   TRESK-1 (*KCNK18*)

7) TRAAK: TWIK-related arachidonic acid-stimulated K+ channel

   TRAAK-1 (*KCNK4*)

The first mammalian K2P channel discovered was TWIK-1 (*KCNK1*), which exhibits high mRNA expression in a wide variety of human tissue, but particularly the brain and heart (Lesage et al., 1996). Interestingly, TWIK-2 (KCNK6) exhibits almost no expression in the brain despite close sequence similarity (Chavez et al., 1999). Within the brain, mRNA from 8 different K2P channels have been found (Aller & Wisden, 2008; Talley, Soló Rzano, Lei, Kim, & Bayliss, 2001).

K2P channels are gated by a wide range of modulatory compounds including lipids, antidepressants, and volatile anesthetics (Florian Lesage, 2003). They are known to be modulated by G-protein-coupled-receptors (Mathie, 2007). As levels of PIP2 decreases due to degradation, TREK channels close. As DAG levels increase, TASK channels close (Bista et al., 2015). Two-pore domain potassium channels are widely expressed throughout the body, setting the resting membrane potential of cells that make up many of the body's organs. In addition to maintaining the resting potential cells, K2P channels regulate cellular excitability, homeostasis, and migration. Impairments in K2P channel function has been linked to pathologies such as depression, hypertension, and cancer (Gotter et al., 2011; Medhurst et al., 2001).

Structure and Pharmacology of K2P Channels

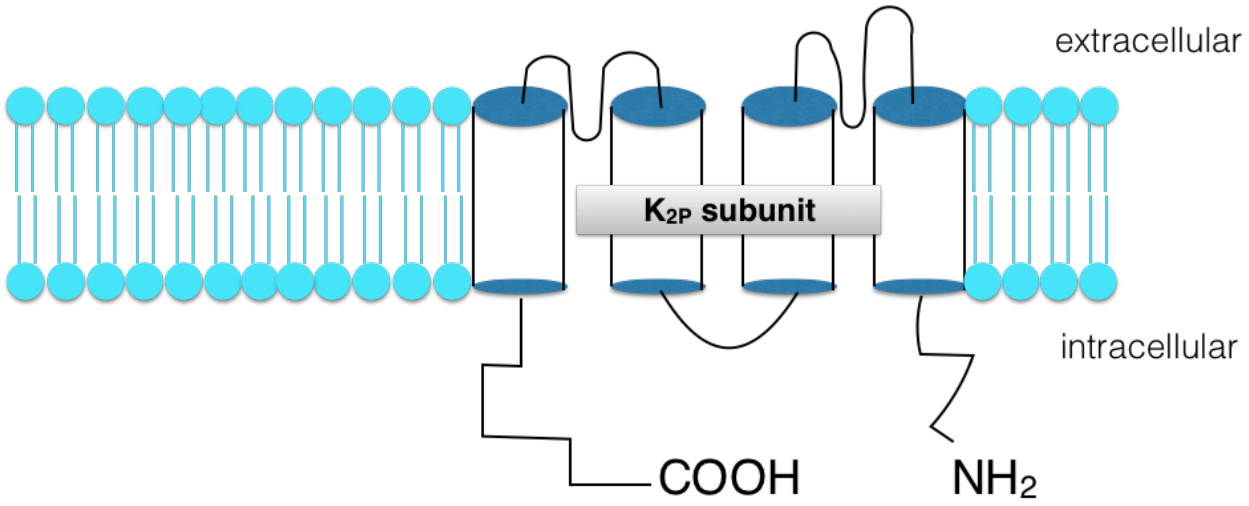

Figure 1. The structure of a single K2P subunit consists of two pore-forming domains (P domains) and four transmembrane domains. Subunits can homodimerize and heterodimerize to form a functional K2P channel.

K^+ channels make up the largest family of ion channels with more than 78 genes encoding subunits. Standard voltage-gated potassium subunits are tetramers with a single pore domain (P domain). P domains are short amino acid segments, nestled between two transmembrane domains, that do not fully cross the membrane. K2P subunits combine to form dimers, each subunit consisting of two P domains (Figure 1). All K^+ channels have four P domains that form the potassium selectivity filter.

Each subunit contains a short intracellular N terminus and large intracellular C terminus. Transmitter inhibition and anesthetic activation requires a region of six amino acids at the interface between the fourth transmembrane domain and the intracellular C terminus (Talley and Bayliss, 2002). For TASK-3, these six amino acids are VLRFLT.

My goal is to elucidate the molecular mechanism underlying the timing of SA in the mouse embryonic hindbrain. Prior work in the lab has shown that SA retraction and silencing is due to increased resting conductance and resting membrane potential hyperpolarization, leading

to decreased cellular excitability (Watari et al., 2013). An increase in expression of K^+ channels that are open at rest and cause membrane hyperpolarization would be the simplest explanation given our physiological data.

K2P channels are a class of background leak channels that drive the membrane potential toward the K+ equilibrium potential (-90mV), reducing excitability. I hypothesize that by allowing membrane hyperpolarization, K2P channels are the molecular switch controlling hindbrain SA. Specifically, I predict that the pattern of K2P channel expression is inversely correlated with the presence of SA in that region (Figure 2).

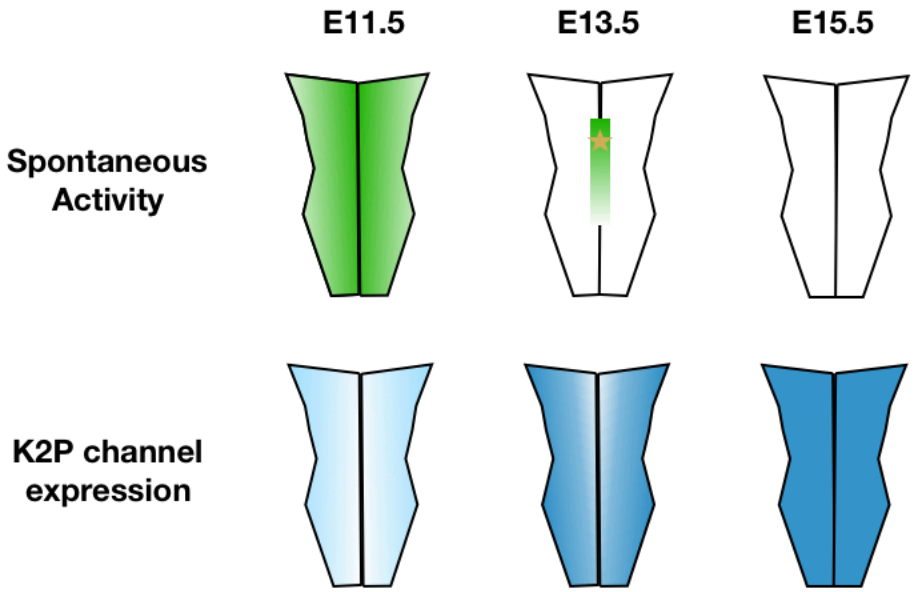

Figure 2. Summary of spatiotemporal characteristic of hindbrain spontaneous activity and hypothesized expression pattern of K2P channels. K2P channel expression is hypothesized to be inversely correlated with hindbrain spontaneous activity. As K2P channels become functionally expressed, potassium conductance increases, driving the resting membrane potential away from the excitability threshold and silencing cells.

RESULTS

Characterization of K2P channel expression in the mouse hindbrain before, during, and after period of active SA

In order to identify the K2P channel that we believe is regulating the spatiotemporal properties of hindbrain SA, I first performed reverse-transcriptase PCR (RT-PCR) of all K2P channels that have ever been shown to be present in the adult or embryonic mouse brain. Of the 15 genes that encode for subunits that then dimerize to form K2P channels, 8 have been identified in the brain (Aller & Wisden, 2008; Talley, Soló Rzano, Lei, Kim, & Bayliss, 2001): TWIK-1 (*KCNK1*), TREK-1 (*KCNK2*), TASK-1 (*KCNK3*), TRAAK-1 (*KCNK4*), TASK-2 (*KCNK5*), TASK-3 (*KCNK9*), TREK-2 (*KCNK10*), and TRESK-2 (*KCNK18*). I chose to perform RT-PCR on tissue taken from E11.5 and E15.5 hindbrain (Figure 3A) to represent a stage where SA is present (E11.5) and extinguished due to membrane hyperpolarization (E15.5). Results of the E11.5 vs E15.5 RT-PCR (Figure 3A) show clear amplification of 4 out of the 8 candidate K2P channels: TWIK-1 (*KCNK1*), TREK-1 (*KCNK2*), TASK-3 (*KCNK9*), and TREK-2 (*KCNK10*). 2 candidate channels had an ambiguous signal at E15.5: TASK-1 (*KCNK3*), TRAAK-1 (*KCNK4*) while the remaining two were absent at both stages.

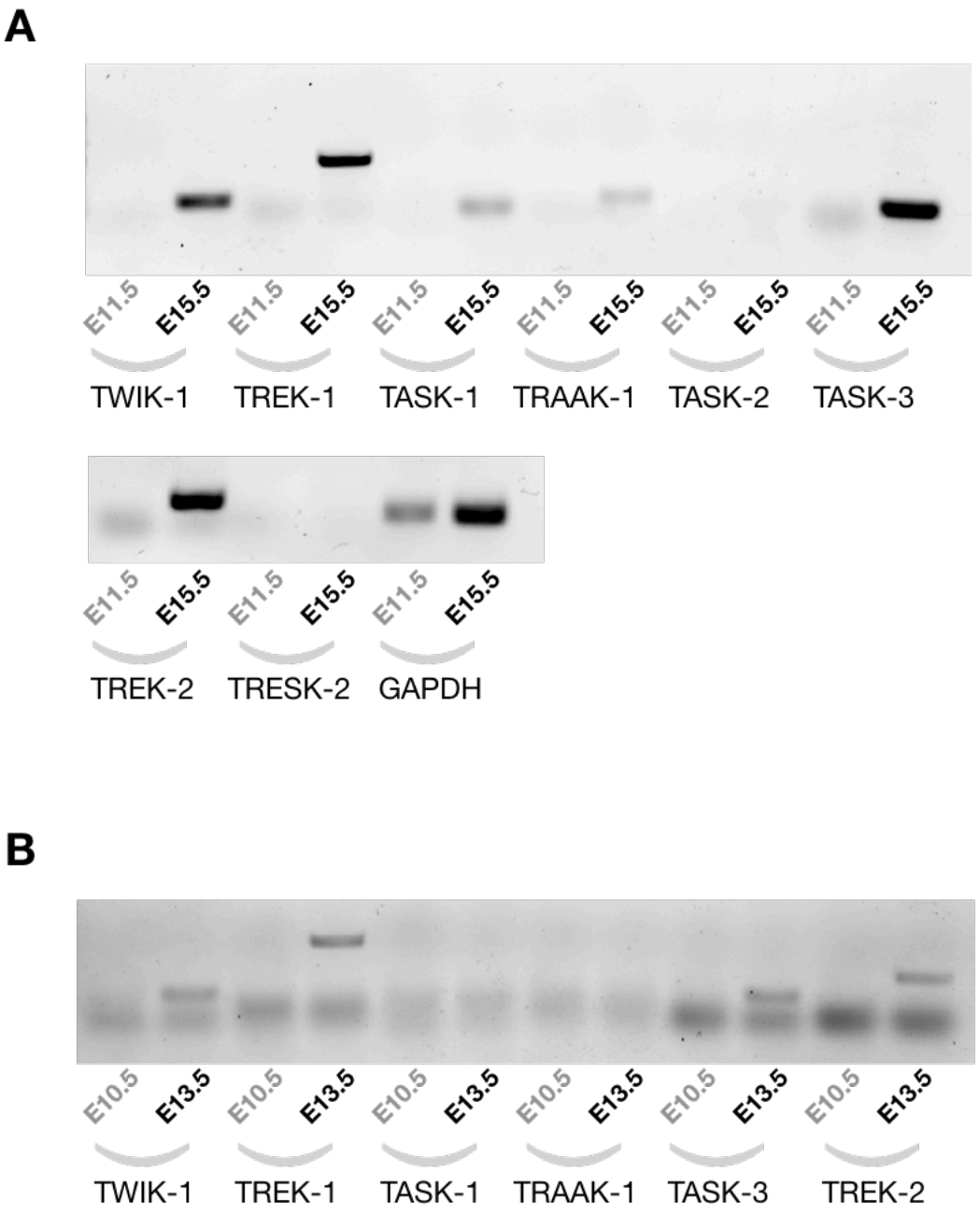

Figure 3. RT-PCR with primers for all K2P channels known to be expressed in mouse brain tissue at (A) E11.5 vs E15.5, and (B) E10.5 vs E13.5.

To further characterize the timeline of K2P channel expression, I performed another RT-PCR using tissue from E10.5 and E13.5 hindbrains (Figure 3B). Based on the results from Figure

3A, I hypothesized that at E10.5 there would be an undetectable amount of K2P channel mRNA, and at E13.5 channels that might be involved in regulating SA would start to emerge since lateral and caudal hindbrain cells have begun to hyperpolarize (Watari et al., 2013). I excluded TASK-2 (*KCNK5*) and TRESK-2 (*KCNK18)* from this experiment since previous runs showed no expression at E15.5. Results of the E10.5 vs E13.5 RT-PCR (Figure 3B) show amplification of the same 4 K2P channels as in previous experiments: TWIK-1 (*KCNK1*), TREK-1 (*KCNK2*), TASK-3 (*KCNK9*), and TREK-2 (*KCNK10*). I hypothesized that at least one of these 4 candidate channels is upregulated in a spatiotemporal manner that coincides with the retraction of hindbrain SA. Because K2P channels have been shown to heterodimerize within and between families (Czirják & Enyedi, 2002; Mi Hwang et al., 2014), there was a reasonable chance that a multiple subunits are responsible for regulating SA.

Further quantification of mRNA levels across various stages of hindbrain development prompted me to perform quantitative PCR (qPCR) of the 4 candidate K2P channels. Hindbrain tissue was taken from E11.5 and E15.5 animals and relative fold change in mRNA levels for each candidate K2P channel was calculated from C_T readouts. When the cDNA was synthesized from entire hindbrain, TASK-3 (*KCNK9*) showed the greatest fold change between E11.5 and E15.5 at 92x (Figure 4B). The second-highest was TWIK-1 (*KCNK1)* at 8x. When the most lateral tissue was discarded during dissection to concentrate the midline tissue, the fold change was greatly enhanced for both TASK-3 (*KCNK9)* at 158x and TWIK-1 (*KCNK1*) at 27x (Figure 4C). This suggests that the upregulation of K2P channels from E11.5 to E15.5 has a greater effect along the midline than across the entire hindbrain, supporting the hypothesis that the midline is the last region to remain spontaneously active because K2P channels do not get expressed along the midline until E15.5.

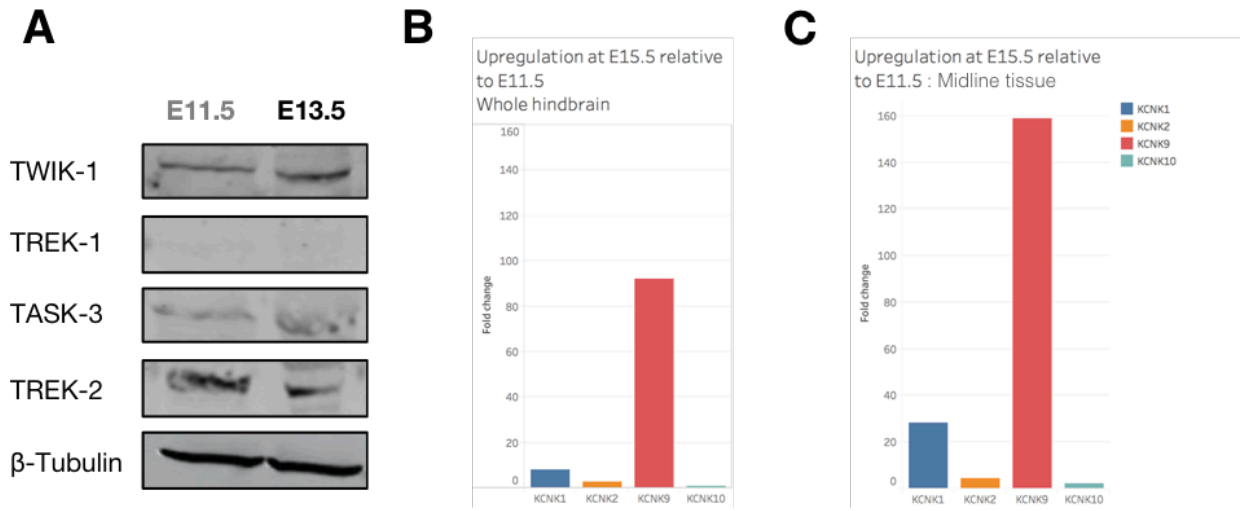

Figure 4. An unsuccessful attempt to identity protein-level expression of K2P channels at E11.5 and E13.5 using Western blots (A). The antibodies used produced low-quality bands, and without the presence of a positive control, the lack of a band for TREK-1 could not actually rule out the absence of the channel in hindbrain tissue. qPCR of mRNA levels of the 4 different K2P channels that showed differential expression between E10.5-15.5 according to RT-PCR results (B, C). Fold change is presented on the y-axis. Of all the channels, TASK-3 (KCNK9) shows the largest fold change over time (92x). This finding is greatly enhanced when midline tissue was isolated (C, KCNK9 is upregulated 158-fold), suggesting the upregulation of KCNK9 is more concentrated along the midline than across the whole hindbrain.

While the expression pattern of K2P channel mRNA supported my hypothesis, I needed to verify that functional protein products are expressed in the same spatiotemporal manner. I first attempted a Western blot of hindbrains taken at E11.5 and E13.5 with antibodies against the 4 candidate channels I identified using RT-PCR. Several attempts proved unsuccessful due to unreliable antibodies, but the results of the blot can be seen in Figure 4A. Protein for 3 of the 4 candidate channels are present at both E11.5 and E13.5. TREK-1 (*KCNK2*) either has no protein expressed at the stages tested or the antibody used was bad. To verify the results the Western blot, and also to visualize protein-level expression *in situ*, I decided to perform

immunohistochemistry (IHC) on sectioned hindbrain tissue. Below is a brief overview of the each of the 4 candidate K2P channels, their known function in the CNS, and a summary of my IHC results.

TWIK-1 (*KCNK1*)

KCNK1 came in second-highest for mRNA fold change at E15.5 vs E11.5 in my qPCR after *KCNK9*. Despite abundant mRNA expression in the mammalian heart, brain, and kidneys, *KCNK1* is one of the several K2P channels that does not produce current (Rajan, Plant, Rabin, Butler, & Goldstein, 2005). Small ubiquitin modifier 1 (SUMO1) colocalizes with *KCNK1* in the plasma membrane and requires Lys274 on *KCNK1* as the site of inactivation (Plant et al., 2010). Mutation of Lys274 to Gln, Arg, Glu, Asp, Cys, or Ala produces a channel that is constitutively active (Plant et al., 2010). Desumoylation by SUMO protease (SENP-1) also activates the channel, and application of SUMO1 to an activated channel resilences it as long as Lys274 is intact (Plant et al., 2010; Rajan et al., 2005). Since TWIK-1 (*KCNK1*) is well-known to be an inactive K2P channel, this rules it out as a potential regulator of hindbrain SA.

TREK-1 (*KCNK2*)

KCNK2 showed very little change in mRNA levels at E15.5 compared to E11.5 (Figure 4 B, C). Immunostaining against *KCNK2* reveals cellular morphology indicative of expression in endothelial cells rather than neurons, neuronal precursors, or glial cells (Figure 5). It has been shown that in the CNS, endothelial TREK-1 (*KCNK2*) regulates leukocyte migration via MAP kinase and the cellular adhesion molecules ICAM1, VCAM1, and PECAM1 (Bittner et al., 2013). Based on my IHC results showing expression in endothelial-looking cells, my qPCR

results showing minor upregulation between E11.5 and E15.5, and published work from other labs revealing a role for the channel in immune-cell trafficking in the CNS, I decided to rule out *KCNK2* as a potential regulator of hindbrain spontaneous activity.

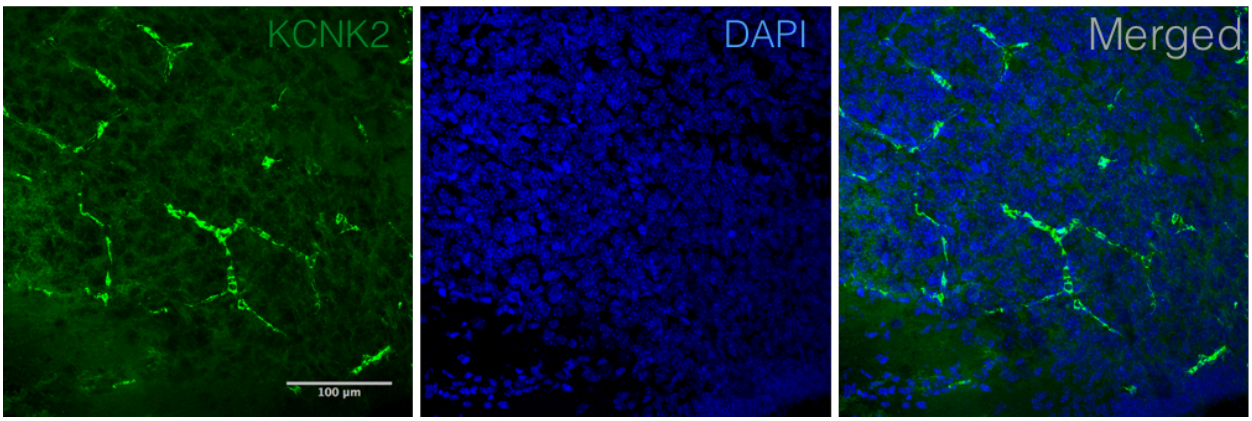

Figure 5. IHC with antibodies against TREK-1 (KCNK2) and DAPI DNA stain at E15.5. The morphology of the cells expressing KCNK2 suggests that these channels are expressed mainly in endothelial cells.

TASK-3 (*KCNK9*)

KCNK9 showed the highest upregulation of the 4 candidate channels at 92-times fold change at E15.5 relative to E11.5 (Figure 4B). Additionally, the fold change becomes even more pronounced when midline tissue was concentrated by discarding the lateral-most tissue during hindbrain dissection (158-fold at E15.5 relative to E11.5, Figure 4C). This suggests that the upregulation seen at later stages of hindbrain development affects the midline more than lateral tissues.

IHC against *KCNK9* shows expression is widely distributed along the lateral hindbrain but progressively shrinks the closer it gets to the midline at E11.5 (Figure 6A). At E15.5, *KCNK9* is expressed uniformly across the hindbrain (Figure 6B). To directly test the hypothesis that cells

that participate in SA lack K2P channels, we recorded directly from midline cells at E11.5, filled the active cell with neurobiotin tracer to track electrically-coupled cells, and co-stained with an antibody against *KCNK9* to visualize the relationship between the leak channel and spontaneously active cells. We confirmed that the cluster of active cells we recorded from did not overlap with *KCNK9* channels, supporting our hypothesis. TASK-3 (*KCNK9*) remains a likely candidate for regulating SA in the mouse hindbrain.

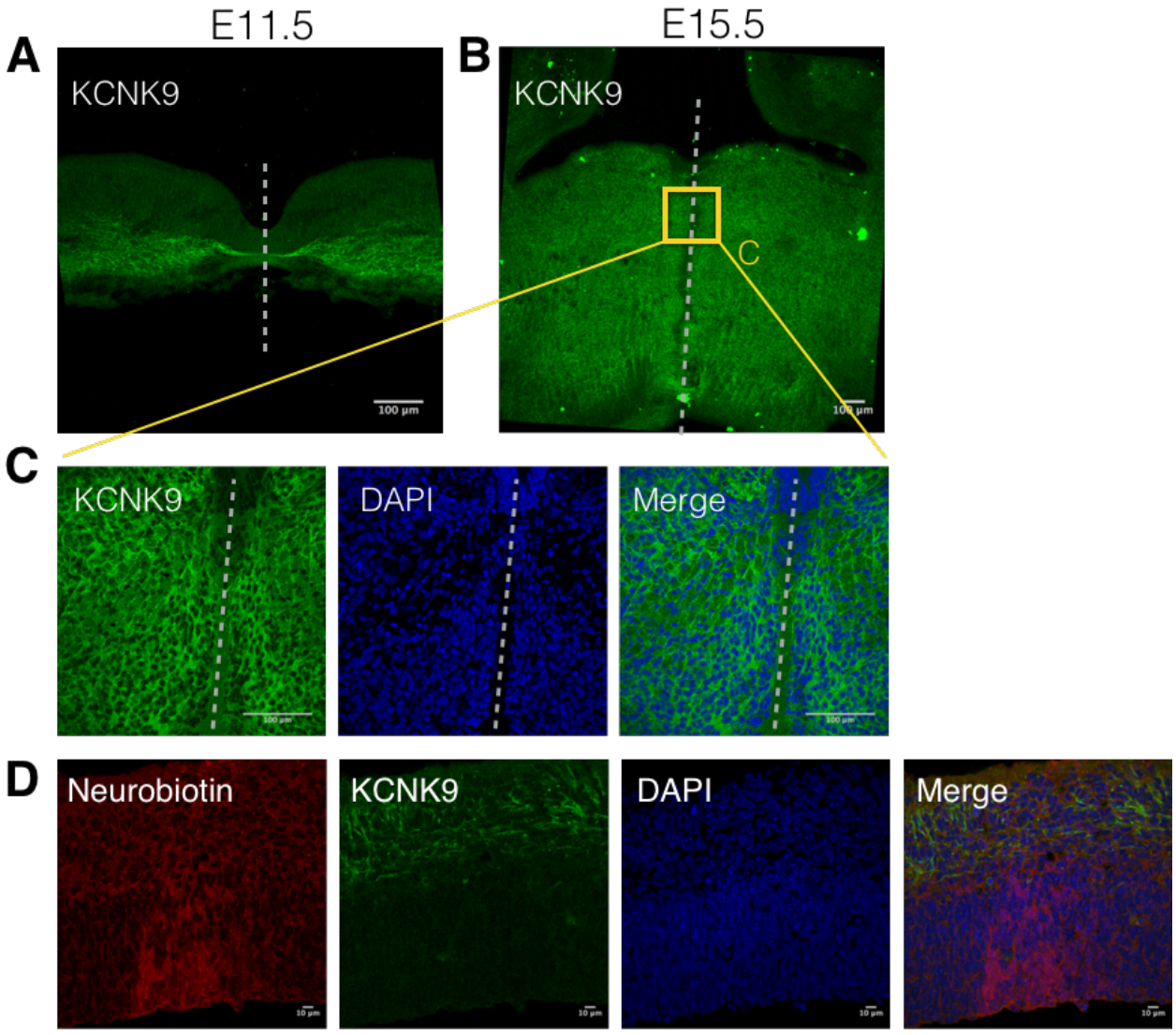

Figure 6. Immunohistochemistry with antibodies against TASK-3 (KCNK9) at E11.5 (A) and E15.5 (B). The midline is shown by the grey dotted line. The yellow box in (B) is magnified (C) to show TASK-3 channels encroaching upon the midline at E15.5 with DAPI DNA stain.

Neurobiotin-filled cells are electrically-coupled by gap junctions. In (D), a whole-cell recording was done and SA was present in the recorded cell. Co-staining with KCNK9 reveals that electrically-coupled active cells do not express the channel.

TREK-2 (*KCNK10*)

qPCR of TREK-2 (*KCNK10*) shows no fold-change at E15.5 relative to E11.5. When entire-hindbrain tissue was used, the fold-change was 0.9 and when midline tissue was concentrated, the fold-change was 1.1 (Figure 4 B, C). A fold-change of 1 means there was the same amount of mRNA across the 2 groups used for comparison. Immunostaining against *KCNK10* shows that the channel is widely distributed at E11.5 and E15.5. The hindbrain midline is the site of densely packed axonal commissures from neurons that send their axons across the midline to coordinate left and right sensory and motor function (Renier et al., 2010). Compared to *KCNK9, KCNK10* is expressed much more highly in these commissures from as early as E11.5. The expression pattern of *KCNK10* does not support a role in regulating hindbrain SA.

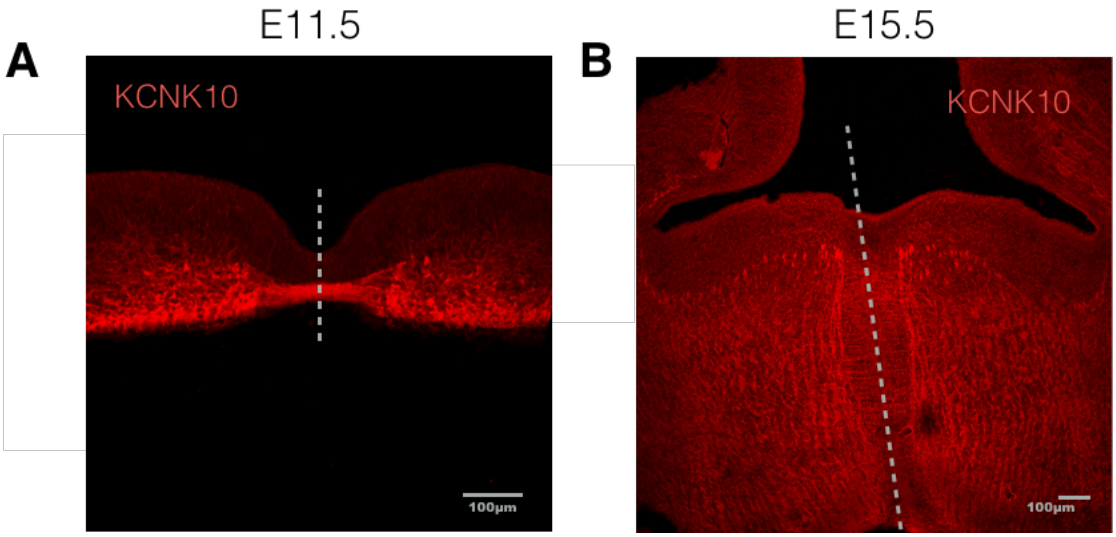

Figure 7. Immunohistochemistry with antibodies against TREK-2 (KCNK10) at E11.5 (A) and E15.5 (B). The midline is shown by the grey dotted line. qPCR results show negligible fold change in mRNA levels at E15.5 relative to E11.5.

Timing of SA in the hindbrain can be altered by blocking KCNK9 pharmacologically

Of the 4 candidate K2P channels identified by RT-PCR, TASK-3 (*KCNK9*) is the most likely channel to be regulating hindbrain SA based on its expression pattern *in situ* and drastic upregulation between E11.5 and E15.5. To directly test whether SA can be altered by changing channel activity, I performed calcium imaging of live hindbrain tissue at E14.5, a stage where SA has just begun to fade across the entire hindbrain due to recent membrane hyperpolarization (Watari et al., 2013). After recording a stable 10-minute baseline recording, I applied the specific TASK-3 channel antagonist, PK-THPP (1-{1-[6-(biphenyl-4-ylcarbonyl)-5,6,7,8-tetrahydropyrido[4,3-d]-pyrimidin-4-yl]piperidin-4-yl}propan-1-one, 1-2 μM). Out of 11 hindbrains tested, 8 showed an increase in spontaneous calcium events. The timecourse of those 8 experiments are shown in Figure 8A. The events did not halt entirely after

washing the drug off with ACSF. It has been previously reported that PK-THPP binds to the intracellular pore of TASK-3, making clearance of the drug difficult (Chokshi, Larsen, Bhayana, & Cotten, 2015). Representative traces from a single calcium-imaging experiment is shown in Figure 8B with the TASK-3 antagonist applied at 10 minutes into the experiment and peak calcium events at 35 minutes. These experiments demonstrate that the period of SA can be prolonged by blocking TASK-3 pharmacologically.

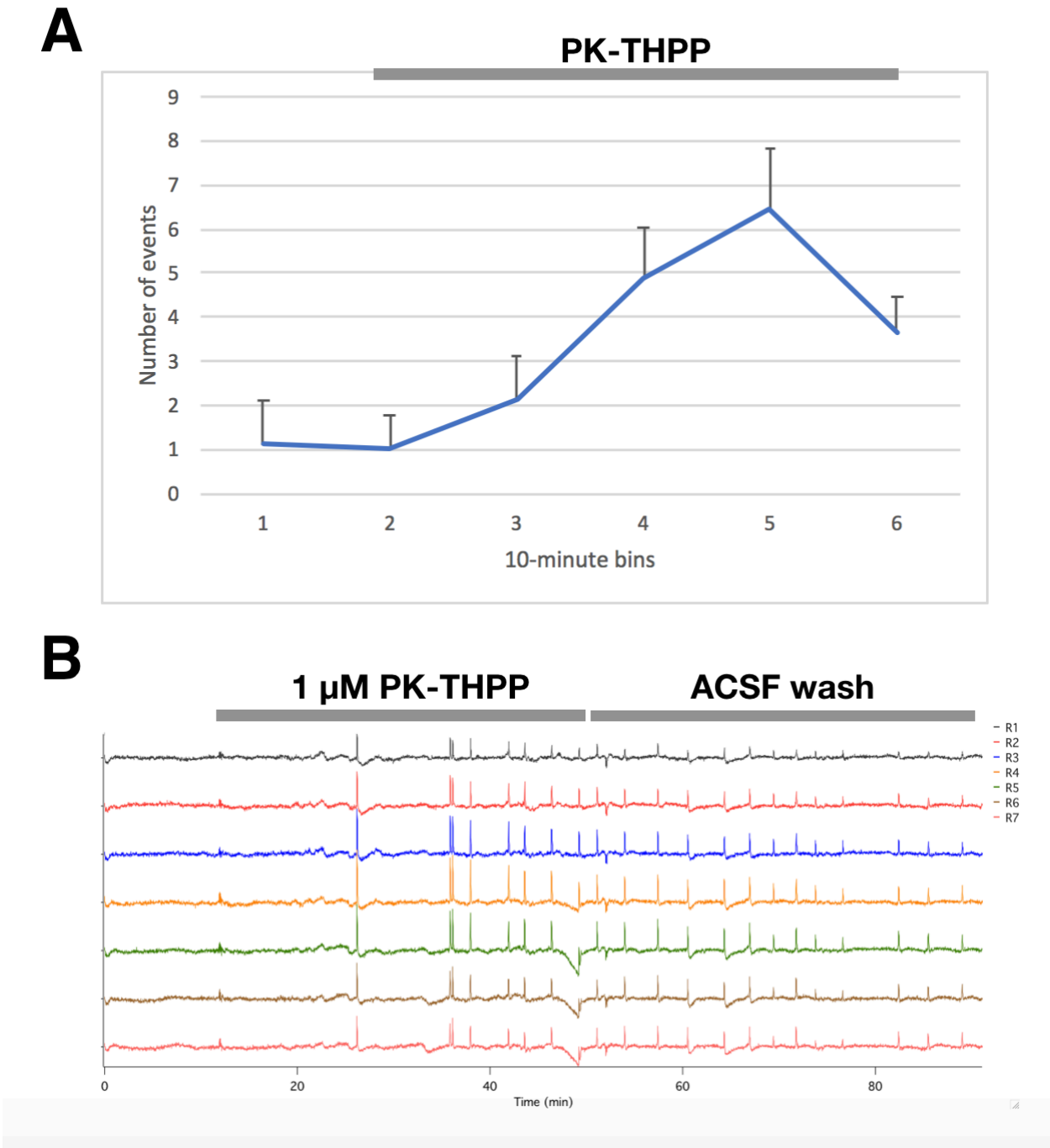

Figure 8. Calcium imaging of E14.5 hindbrains with the specific TASK-3 antagonist, PK-THPP, used at 1-2 µM (n=8) (A). The entire recorded session is broken down into 10-minute bins for frequency analysis. After a 10-minute baseline recording, the drug was perfused onto the tissue. Application of the TASK-3 antagonist triggered an increase in spontaneous events that did not wash out after the drug was removed. Representative traces of change in fluorescence in 7 regions of interest spanning the hindbrain midline (B).

CB1-receptor agonist methanandamide alters SA, possibly through TASK-3 mediation

Methanandamide is a non-hydrolysable analogue of anandamide. Its role in regulating hypothermia and analgesia have been established as acting through CB1 receptors, but other effects such as locomotion and ataxia are believed to be CB1-independent. Mouse TASK-3 shows 50% inhibition by 3 μM methanandamide in transfected cells during whole-cell voltage-clamp recordings (Veale, Buswell, Clarke, & Mathie, 2009). Human TASK-3 and TASK-1 were significantly more inhibited by the same concentration of methanandamide. Preliminary results show that SA is upregulated at E14.5 upon application of methanandamide (5 μM, not shown) during calcium imaging. Similar to PK-THPP, removing the drug from the bath does not eliminate spontaneous activity. Methanandamide and PK-THPP might share a similar binding site at the intracellular pore of TASK-3.

Investigating the effects of genetic knockout of KCNK9 on SA

We have recently obtained a genetic knockout mouse line for *KCNK9* and are in the processing of testing the animals for aberrant SA but it is still too early to draw conclusions. In addition to performing calcium imaging experiments on the knockout animals, we are using IHC to confirm that knockout animals do not express *KCNK9* and are looking at differences in cellular morphology between knockout animals and wild-type littermates.

Transcriptome biological pathways enrichment analysis

The intent behind my dissertation project was that by searching for the molecular regulators of hindbrain SA, we would be able to shed light on the biological pathways that are mediated by SA. I decided to approach this question by mining human transcriptome data from

the Allen Brain Institute (www.brainspan.org). This approach would begin to answer two important questions raised by my molecular results: 1) is the mouse a reliable model animal for studying brain development? and 2) can examining the expression pattern of TASK-3/*KCNK9* help us understand how SA regulates development?

To answer the first question, I needed to show that TASK-3/*KCNK9* is also upregulated in humans during embryonic development, and that the upregulation of TASK-3/*KCNK9* is correlated with genes and pathways that relate to SA. According to the Allen Brain Institute's Transcriptome Database, BrainSpan, *KCNK9* is highly upregulated between post-conceptual weeks 16-24. Enrichment analysis of the top 2000 correlated genes shows that the following pathways are enriched among those genes: regulation of membrane potential (73 genes), receptor localization of synapse (11 genes), cellular response to calcium ion (20 genes), metencephalon development (22 genes).

To understand how SA regulates hindbrain development, I decided investigate enriched biological pathways that are not directly involved in regulating cellular activity: muscle processes (Figure 9) and learning and memory (Figure 10). The heatmaps show *KCNK9*-correlated genes clustered by expression level. Because genes with a similar expression pattern are more likely to be co-regulated, this is an attempt to lay the foundation for future work to investigate how *KCNK9* regulates brain development. A summary of how *KCNK9* expression might contribute to learning and memory is highlighted in the discussion. Among the 45 muscle-related genes, one gene that stands out is SMN1. In humans, there are 2 SMN genes (SMN1 and SMN2). Mutations in both genes are embryonic lethal, yet a mutation in a single gene is linked to spinal muscular atrophy. It has been shown that muscle biopsies of those with *KCNK9* imprinting syndrome resemble those with spinal muscular atrophy (Barel et al., 2008). How

these two genes might be co-regulated is an interesting topic for future studies. Lastly, several enriched pathways point to an association between TASK-3/*KCNK9* and neuronal projection development: dendrite development (28 genes), axon development (60 genes), axon extension (20 genes). IHC using tissue from *KCNK9* knockout animals would be a good technique to explore this topic.

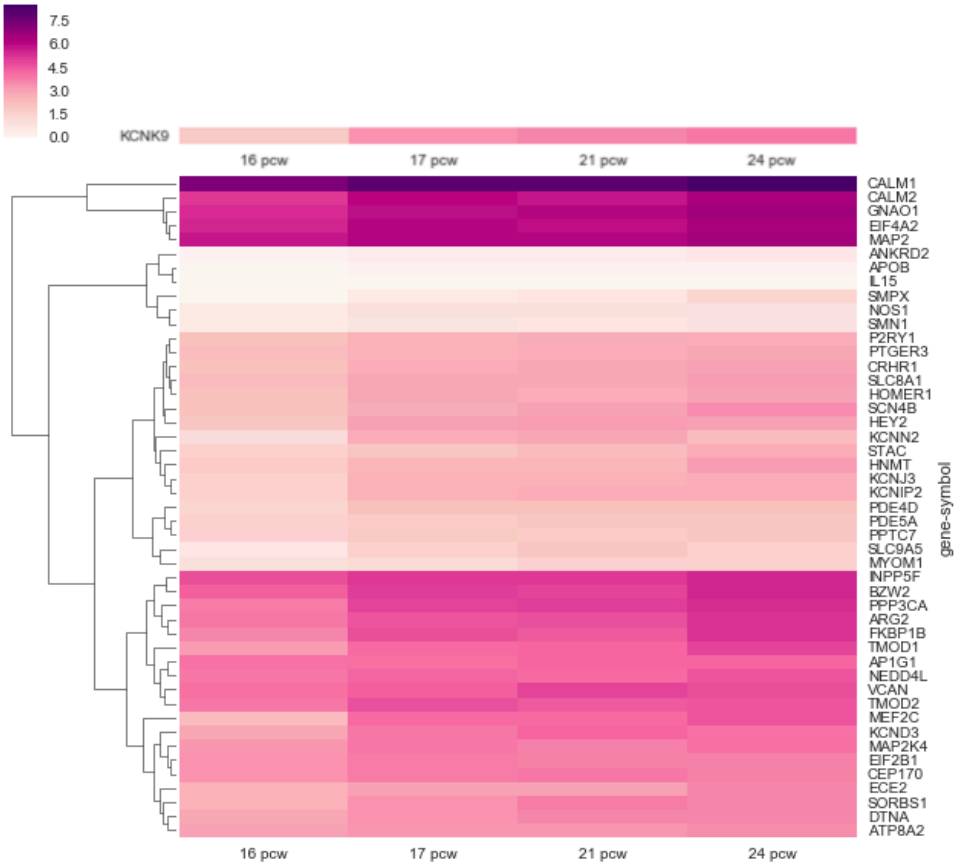

Figure 9. Muscle-processes associated genes that are highly correlated with human *KCNK9* expression between 16-24 pcw.

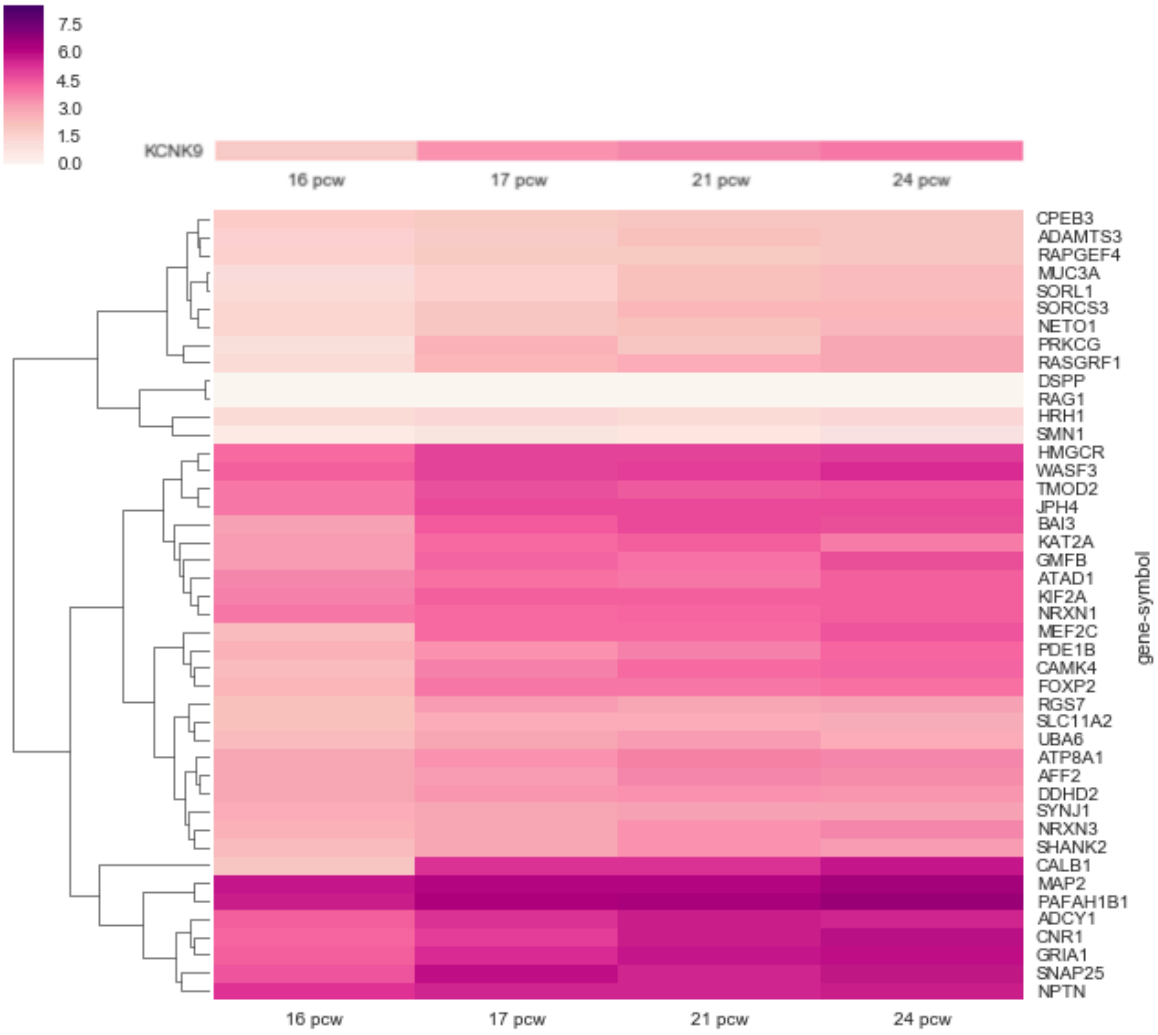

Figure 10. Learning and memory associated genes that are highly correlated with human *KCNK9* expression between 16-24 pcw.

DISCUSSION

The question I set out to answer at the beginning of my PhD work was, "how is spontaneous activity contributing to hindbrain development?". In the process of figuring out my original aim, I made the following discoveries: 1) TWIK-1 mRNA is found in the hindbrain as early as E11.5, which was previously unreported, 2) though it was previously known that TREK-1 mRNA is found in the embryonic mouse hindbrain, my immunohistochemistry staining shows widespread expression in endothelial cells compared to neurons, suggesting a role in regulating vasculature rather than neural development, 3) TASK-3 mRNA and protein are upregulated in a spatiotemporal matter that could account for the hyperpolarization of resting membrane potential leading to retraction and cessation of hindbrain spontaneous activity, and 4) cessation of hindbrain spontaneous activity can be pharmacologically reversed by applying the selective TASK-3 antagonist, PK-THPP.

Behavioral Characterization of TASK-3 Knockout Mice

Phenotypic analysis of TASK-3 knockout mice have been extensively performed by several research labs. Linden et al (2007) used the SHIRPA protocol for behavioral assessment and found largely normal behavior in adult TASK-3 knockout animals, including normal exploratory behavior in the open field test, normal levels of anxiety in the elevated plus-maze and light-dark box, and normal thermal nociception in the tail-flick test and hot plate. When the sex of the animal was taken into account, TASK-3 knockout females displayed working memory impairment in the Morris Water Maze probe trials, while male TASK-3 knockout and male wild type animals had similar performance. This was measured by counting the number of visits a

mouse made to the area where a submerged platform was previously hidden. The same group also found aberrant responses to volatile anesthetics in TASK-3 knockout animals, which needed a higher concentration of halothane to induce the loss of the tail-withdrawal reflex. In addition to halothane, they also found a reduced sensitivity to the analgesic effects of CB1 agonist, WIN55212-2.

Several groups have reported that TASK-3 knockout mice are hyperactive relative to wild type animals, but only in the dark phase of the light cycle , suggesting a role for TASK-3 in regulating circadian rhythm activity (Gotter et al., 2011; Linden et al., 2007). Gotter et al. (2011) also found working memory impairment when they tested knockout animals during the rodents' inactive phase but not when they performed the same test in the active/dark phase.

Finally, the properties of K2P channels that allow for its modulation by a diverse array of compounds and agents have prompted the question of their role in sensory perception. It has been shown that 3 different K2P channels (*KCNK3, KCNK9, KCNK18*) mediate the numbing sensation caused by ingesting Szechuan peppers (Bautista et al., 2008). *KCNK9* has also been implicated in sensing cold temperatures, as knocking out the gene results in hypersensitivity to acetone and a dry ice pellet pressed against glass (Morenilla-Palao et al., 2014).

Role of TASK channels in ischemia

TASK stands for TWIK-related Acid-Sensitive K^+ channel. During brain ischemia, extracelluar pH can decrease to as low as 6.0 (Bista et al., 2015). Ischemia is often accompanied by strong, prolonged membrane depolarization and excitotoxity. Neuronal populations that express both TASK and HCN are protected from cellular damage due to the opposing effects

acidic extracellular pH has on these two classes of channels. TASK channels depolarize cellular membrane potential when closed while HCN channels hyperpolarize.

Pharmacological treatments for KCNK9-associated disorders

Birk-Barel Syndrome, also known as *KCNK9* imprinting syndrome, is a result of a missense mutation in the maternal copy of *KCNK9* (Barel et al., 2008). Due to paternal silencing of this gene, a mutation in the maternal copy results in the disorder, regardless of whether the paternal copy is affected. A mutation in the paternal copy alone has no affect. Clinical presentations of the disorder include delayed development, moderate to severe levels of intellectual disability, hyperactivity, feeding difficulties throughout infancy and up to puberty, and hypotonia with proximal muscle weakness. Facial dysmorphisms include a narrow, elongated face with reduced facial movements. The disorder was identified and mapped to chromosome 8q24 by Barel et al. (2008) using genome-wide linkage analysis of a single Israeli Arab family with seven affected individuals. Unrelated patients were later identified using exome sequencing (Graham Jr et al., 2016). The *KCNK9* mutation reduces its outward current by 85%.

Potassium leak channels are crucially important because they regulate excitability and are highly modulated by biological as well as pharmacological compounds. Using cultured cells that express the same mutated form of *KCNK9* that results in Birk-Barel Syndrome, Veale et al. (2014) showed that a class of non-steroidal anti-inflammatory drugs containing fenamic acid can be used to enhance the current of the mutated channel. This recovery of the *KCNK9* current by an already FDA-approved drug led to a clinical trial two years later, suggesting that Birk-Barel Syndrome is a treatable disorder, although these results are preliminary (Graham Jr et al., 2016).

In the clinical study, two patients were treated with oral mefanamic acid starting at 14 months and 18 months of age. The patients' parents reported increased stamina and better communication when the children were on the drug than when they were taken off the drug.

Although mouse and human brain vary drastically due to differences in developmental timescale, mouse has been used extensively as a model for human brain development. The following discoveries about *KCNK9* have been made using rodents as a model animal: *KCNK9* mRNA is found in rat facial motoneurons, where it is thought to contribute to neonatal facial motoneuron excitability (Larkman & Perkins, 2005). *KCNK9* knockout mice are hyperactive, have impaired motor skills, show poor performance in working memory and spatial learning tasks compared to wild-type mice (Linden et al., 2007), phenotypes that mirror the symptoms of Birk-Barel Syndrome.

Methods

Animals

Swiss-Webster mice were either bred in lab or purchased from Envigo. Females of breeding pairs were checked daily for the presence of a vaginal plug. Timed-pregnant mice were used at stages E10.5-15.5 for the experiments outlined in this thesis. Embryos were removed in carbogen (95% O_2/5% CO_2)-bubbled modified artificial cerebrospinal fluid (ACSF) containing (in mM): 119 NaCl, 2.5 KCl, 1.3 $MgCl_2$, 2.5 $CaCl_2$, 1 NaH_2PO_4, 26 $NaHCO_3$, 30 glucose.

TASK-3 mutant animals were a gift from Alistair Mathie and the University of Kent. Information on the generation of the TASK-3 knockout line can be found in Brickley et al. (2007). Animals were maintained as heterozygotes on a C57BL/6 background. Due to genomic

imprinting of the gene that encodes for the TASK-3 channel, *KCNK9,* only the maternal allele gets expressed. Therefore, to characterize the knockout phenotype, we used heterozygous animals that inherited the – allele from the mother. Using a breeding strategy of WT males crossed to +/- females, our litters yielded 50% WT animals (control) and 50% +/- animals with no functional TASK-3 channels. We will call these animals TASK-3 knockouts since the single expressed allele has a targeted deletion of *KCNK9*.

Calcium Imaging

Animals used for calcium imaging experiments were first checked for the presence of a heartbeat. Hindbrains were dissected, incubated with fluo-8 calcium indicator and pluronic F-127 for 15-20 minutes, rinsed, placed into a glass-bottomed experimental chamber, and held in place by a slice anchor (Warner Instruments). MetaFluor software (Universal Imaging/Molecular Devices) was used to measure change in fluorescence of up to 48 regions of interest (ROIs). Calcium traces were later visualized and analyzed in Igor Pro 6 (Wavemetrics, Inc.). Oxygenated ACSF was perfused at a rate of 1 ± 0.3 ml min^{-1} for the duration of the experiment. The selective TASK-3 channel antagonist, PK-THPP (Sigma Aldrich, SML1326), was used at 1-2 μM. Forskolin (Santa Cruz, sc-3562) was applied at 10 μM to increase levels of cAMP and activate the PKA pathway.

Electrophysiology

Whole-cell recordings of midline neurons were performed as previously described (Watari et al., 2013). Patch electrodes were filled with internal solution containing neurobiotin at 10 mg ml^{-1} to visualize cells that are coupled to the recorded cell by gap junctions. If spontaneous activity was

present during the recording, the hindbrain was fixed with 4% PFA for processing with a streptavidin reaction to visualize the group of cells that participated in spontaneous activity.

Immunohistochemistry

Dissected hindbrains were fixed with cold 4% PFA for 20-40 minutes and cast in Tissue-Tek OCT (VWR Scientific). Hindbrains were sliced in a cryostat into 30 μm sections mounted directly onto glass slides treated with Vectabond (Vector Laboratories). Sections were rinsed 5X with PBS-TX, blocked with 10% NGS for 1 hour, and incubated for 1-3 nights with primary antibodies. Secondary antibody was applied for 2 hours followed by a 10-minute DAPI application at 1:1000. The following primary antibodies were used: rabbit anti-TWIK1 (1:200, Sigma Aldrich, K0390), rabbit anti-TASK-3 (1:100, Alomone Labs, #APC-044), rabbit anti-TREK-2 (1:200, Sigma Aldrich, P5122). The following secondary antibodies were used: Alexa Fluor 488-conjugated goat anti-rabbit (1:200, ThermoFisher, #A-11008), Alex Fluor 594-conjugated streptavidin (1:1000, Invitrogen/ThermoFisher).

Western Blots

Hindbrains of E11.5 and E13.5 animals were dissected and flash frozen with liquid nitrogen. 300μL of Tissue-PE LB Buffer (G-Biosciences) was added to each hindbrain prep prior to tissue lysis. Protease inhibitors were added at 1-10% concentration. The tissue was then placed on a rotating plate for 2 hours at 4ºC, centrifuged at 12000rpm for 20 minutes, and pellet was discarded. 2x Laemmli buffer was added to each tube. To reduce and denature, each prep was boiled at 100ºC for 5 minutes. Equal amounts of protein (20-30μg) were loaded into a 10% SDS-PAGE gel and blotted onto PVDF membranes.

The following primary antibodies were used: monoclonal anti-beta-tubulin antibody (1:1000, ThermoFisher, BT7R, #MA5-16308), rabbit anti-TWIK1 (1:200, Sigma Aldrich, K0390), rabbit anti-TREK-1 (1:200, Alomone Labs, #APC-047), rabbit anti-TASK-3 (1:200, Alomone Labs, #APC-044), rabbit anti-TREK-2 (1:200, Sigma Aldrich, P5122), goat anti-TREK-1 (1:200, Santa Cruz, sc-11557), goat anti-TASK-3 (1:200, Santa Cruz, sc-11322). The following secondary antibodies were used: Alexa Fluor 680-conjugated donkey anti-goat (1:10,000, Jackson Laboratory, #705-625-147), Alexa Fluor 680-conjugated goat anti-rabbit (1:10,000, Jackson Laboratory #111-625-144).

Real-time quantitative PCR

First-strand cDNA was synthesized from RNA isolated from mouse hindbrains at E10.5-15.5 using iScript cDNA synthesis kit (Bio-Rad). TaqMan primers specific to each K_2P channel were used along with GAPDH as a housekeeping gene control (ThermoFisher). The qPCR reaction was performed using TaqMan Gene Expression Master Mix (ThermoFisher, #4369016) in a StepOnePlus Real Time PCR System. The following equation was used to calculate fold change:

$$\textbf{Fold change} = 2^{-\Delta(\Delta CT)},$$

$$\text{where } \Delta C_T = C_{T,\text{target}} - C_{T,\text{GAPDH}}$$

$$\text{and } \Delta(\Delta C_T) = \Delta C_{T,E15.5} - \Delta C_{T,E11.5}$$

Reverse Transcriptase PCR

mRNA was isolated from dissected hindbrain tissue using TRIzol (Invitrogen) and chloroform , washed with 70% ethanol, and stored in RNAse free H_2O. First-strand cDNA was synthesized using iScript cDNA synthesis kit (Bio-Rad). Primer sequences are listed in the appendix.

Human Developmental Transcriptome Data Analysis

Transcriptome data was downloaded from the Allen Brain Institute's BrainSpan project (www.brainspan.org). A gene search for *KCNK9* restricted to hindbrain-derived tissues (cerebellum, cerebellar cortex) and prenatal stages founded that the period of highest upregulation was between 16-24 pcw. Further stage restriction yielded 52376 genes ordered by correlation co-efficient. The top 2000 correlated genes had r-values between 1 and 0.801. After removing pseudogenes and unnamed genes, 1474 genes remained. The 1474 remaining genes were put into the Gene Ontology Consortium's Enrichment Analysis tool (http://www.geneontology.org/). Gene expression level heatmaps were made using Python 3.0.

List of primers

Primers for genotyping *KCNK9* transgenic mice

Forward 5'-TCTGTCCCGGCTACCGATCCTGC-3'

Reverse 5'-TTCCGTGGGCGCAGCGGGTTCCGC-3'

Primers for reverse-transcriptase PCR

KCNK1 Forward 5'-CTCAGCAACGCCTCGGGGAAT-3'

KCNK1 Reverse 5'-TGAACGGGATGCCAATGACAGAG-3'

KCNK2 Forward 5'-TTCCCCTCTTTGGCTTTCTACTG-3'

KCNK2 Reverse 5'-CCTCGTTTCCTTGAACTCGGC-3'

KCNK3 Forward 5'-TCATCACCACAATCGGCTAT-3'

KCNK3 Reverse 5'-AGCGCGTAGAACATGCAGAA-3'

KCNK4 Forward 5'-TGTAGGCTTTGGCGATTATGT-3'

KCNK4 Reverse	5’-TGAGGCCACCCATCTCT-3’
KCNK5 Forward	5’-CTATTCCTTCATCACCATCTC-3’
KCNK5 Reverse	5’-AGCCCCAGGTAGATCCAAA-3’
KCNK9 Forward	5’-AAGCCGAAGAAGTCCGTCTCAGAG-3’
KCNK9 Reverse	5’-CCGATAGTTGTGATGACAGTGATGG-3’
KCNK10 Forward	5’-ATCTTCGTGGTGGTCGTGGTCTAC-3’
KCNK10 Reverse	5’-TGGTTGTGATGACTGTCCCAGC-3’
KCNK18 Forward	5’-CTCACTTCTTCCTCTTCTTCTC-3’
KCNK18 Reverse	5’-TAGCAAGGTAGCGAAACCTCT-3’
GAPDH Forward	5’-CGCATCTTCTTGTGCAGT-3’
GAPDH Reverse	5’-AATGAAGGGGTCGTTGATGG-3’

REFERENCES

Aller, M. I., & Wisden, W. (2008). Changes in expression of some two-pore domain potassium channel genes (KCNK) in selected brain regions of developing mice. *Neuroscience*, *151*(4), 1154–1172. https://doi.org/10.1016/j.neuroscience.2007.12.011

Barel, O., Shalev, S. A., Ofir, R., Cohen, A., Zlotogora, J., Shorer, Z., … Birk, O. S. (2008). Maternally Inherited Birk Barel Mental Retardation Dysmorphism Syndrome Caused by a Mutation in the Genomically Imprinted Potassium Channel KCNK9, 193–199. https://doi.org/10.1016/j.ajhg.2008.07.010.

Bautista, D. M., Sigal, Y. M., Milstein, A. D., Garrison, J. L., Zorn, J. a, Tsuruda, P. R., … Julius, D. (2008). Pungent agents from Szechuan peppers excite sensory neurons by inhibiting two-pore potassium channels. *Nature Neuroscience*, *11*(7), 772–779. https://doi.org/10.1038/nn.2143

Bista, P., Cerina, M., Ehling, P., Leist, M., Pape, H.-C., Meuth, S. G., & Budde, T. (2015). The role of two-pore-domain background K+ (K2P) channels in the thalamus. *Pflügers Archiv - European Journal of Physiology*, *467*(5), 895–905. https://doi.org/10.1007/s00424-014-1632-x

Bittner, S., Ruck, T., Schuhmann, M. K., Herrmann, A. M., Maati, H. M. ou, Bobak, N., … Meuth, S. G. (2013). Endothelial TWIK-related potassium channel-1 (TREK1) regulates immune-cell trafficking into the CNS. *Nature Medicine*, *19*(9), 1161–1165. https://doi.org/10.1038/nm.3303

Chavez, R. A., Gray, A. T., Zhao, B. B., Kindler, C. H., Mazurek, M. J., Mehta, Y., … Yost, C. S. (1999). TWIK-2, a new weak inward rectifying member of the tandem pore domain potassium channel family. *The Journal of Biological Chemistry*, *274*(12), 7887–7892.

https://doi.org/10.1074/JBC.274.12.7887

Chokshi, R. H., Larsen, A. T., Bhayana, B., & Cotten, J. F. (2015). Breathing Stimulant Compounds Inhibit TASK-3 Potassium Channel Function Likely by Binding at a Common Site in the Channel Pore. *Molecular Pharmacology*, *88*(5), 926–934. https://doi.org/10.1124/mol.115.100107

Clause, A., Kim, G., Sonntag, M., Weisz, C. J. C., Vetter, D. E., Rűbsamen, R., & Kandler, K. (2014). The Precise Temporal Pattern of Prehearing Spontaneous Activity Is Necessary for Tonotopic Map Refinement. *Neuron*, *82*(4), 822–835. https://doi.org/10.1016/J.NEURON.2014.04.001

Czirják, G., & Enyedi, P. (2002). Formation of functional heterodimers between the TASK-1 and TASK-3 two-pore domain potassium channel subunits. *The Journal of Biological Chemistry*, *277*(7), 5426–5432. https://doi.org/10.1074/jbc.M107138200

Feliciangeli, S., Chatelain, F. C., Bichet, D., & Lesage, F. (2014). The family of K2P channels: salient structural and functional properties. *The Journal of Physiology*, *0*(November 2014), 1–17. https://doi.org/10.1113/jphysiol.2014.287268

Gotter, A. L., Santarelli, V. P., Doran, S. M., Tannenbaum, P. L., Kraus, R. L., Rosahl, T. W., … Renger, J. J. (2011). TASK-3 as a potential antidepressant target. *Brain Research*, *1416*, 69–79. https://doi.org/10.1016/J.BRAINRES.2011.08.021

Hunt, P. N., McCabe, A. K., & Bosma, M. M. (2005). Midline serotonergic neurones contribute to widespread synchronized activity in embryonic mouse hindbrain. *The Journal of Physiology*, *566*(Pt 3), 807–819. https://doi.org/10.1113/jphysiol.2005.089581

Jr, J. M. G., Zadeh, N., Kelley, M., Tan, E. S., Liew, W., Tan, V., … Al, G. E. T. (2016). KCNK9 Imprinting Syndrome — Further Delineation of a Possible Treatable Disorder,

2632–2637. https://doi.org/10.1002/ajmg.a.37740

Krumlauf, R., & Keynes, R. (1994). Box Genes and Regionalization of the Nervous System. *Annual Review of Neuroscience*, *17*, 109–132.

Larkman, P. M., & Perkins, E. M. (2005). A TASK-like pH- and amine-sensitive ' leak ' K + conductance regulates neonatal rat facial motoneuron excitability in vitro, *21*(August 2004), 679–691. https://doi.org/10.1111/j.1460-9568.2005.03898.x

Lesage, F. (2003). Pharmacology of neuronal background potassium channels. *Neuropharmacology*, *44*(1), 1–7. https://doi.org/10.1016/S0028-3908(02)00339-8

Lesage, F., Guillemare, E., Fink, M., Duprat, F., Lazdunski, M., Romey, G., & Barhanin, J. (n.d.). TWIK-1, a ubiquitous human weakly inward rectifying K+ channel with a novel structure. *The EMBO Journal*, *15*(5), 1004–1011. https://doi.org/10.1002/J.1460-2075.1996.TB00437.X

Linden, A.-M., Sandu, C., Aller, M. I., Vekovischeva, O. Y., Rosenberg, P. H., Wisden, W., & Korpi, E. R. (2007). TASK-3 Knockout Mice Exhibit Exaggerated Nocturnal Activity, Impairments in Cognitive Functions, and Reduced Sensitivity to Inhalation Anesthetics. *Journal of Pharmacology and Experimental Therapeutics*, *323*(3), 924–934. https://doi.org/10.1124/jpet.107.129544

Mathie, A. (2007). Neuronal two-pore-domain potassium channels and their regulation by G protein-coupled receptors. *The Journal of Physiology*, *578*(Pt 2), 377–385. https://doi.org/10.1113/jphysiol.2006.121582

Medhurst, A. D., Rennie, G., Chapman, C. G., Meadows, H., Duckworth, M. D., Kelsell, R. E., … Pangalos, M. N. (2001). Distribution analysis of human two pore domain potassium channels in tissues of the central nervous system and periphery. *Molecular Brain Research*,

86(1–2), 101–114. https://doi.org/10.1016/S0169-328X(00)00263-1

Mi Hwang, E., Kim, E., Yarishkin, O., Ho Woo, D., Han, K.-S., Park, N., … Park, J.-Y. (2014). A disulphide-linked heterodimer of TWIK-1 and TREK-1 mediates passive conductance in astrocytes. *Nature Communications*, *5*(1), 3227. https://doi.org/10.1038/ncomms4227

Moody, W. J., & Bosma, M. M. (2005). Ion Channel Development , Spontaneous Activity , and Activity-Dependent Development in Nerve and Muscle Cells, 883–941. https://doi.org/10.1152/physrev.00017.2004.

Morenilla-Palao, C., Luis, E., Fernández-Peña, C., Quintero, E., Weaver, J. L., Bayliss, D. A., & Viana, F. (2014). Ion Channel Profile of TRPM8 Cold Receptors Reveals a Role of TASK-3 Potassium Channels in Thermosensation. *Cell Reports*, *8*(5), 1571–1582. https://doi.org/10.1016/J.CELREP.2014.08.003

Plant, L. D., Dementieva, I. S., Kollewe, A., Olikara, S., Marks, J. D., & Goldstein, S. A. N. (2010). One SUMO is sufficient to silence the dimeric potassium channel K2P1. *Proceedings of the National Academy of Sciences of the United States of America*, *107*(23), 10743–10748. https://doi.org/10.1073/pnas.1004712107

Rajan, S., Plant, L. D., Rabin, M. L., Butler, M. H., & Goldstein, S. A. N. (2005). Sumoylation Silences the Plasma Membrane Leak K+ Channel K2P1. *Cell*, *121*(1), 37–47. https://doi.org/10.1016/J.CELL.2005.01.019

Renier, N., Schonewille, M., Giraudet, F., Badura, A., Tessier-Lavigne, M., Avan, P., … Chédotal, A. (2010). Genetic Dissection of the Function of Hindbrain Axonal Commissures. *PLoS Biology*, *8*(3), e1000325. https://doi.org/10.1371/journal.pbio.1000325

Spitzer, N. C. (2012). Activity-dependent neurotransmitter respecification, *13*(February). https://doi.org/10.1038/nrn3154

Talley, E. M., Soló Rzano, G., Lei, Q., Kim, D., & Bayliss, D. A. (n.d.). CNS Distribution of Members of the Two-Pore-Domain (KCNK) Potassium Channel Family. Retrieved from http://www.jneurosci.org/content/jneuro/21/19/7491.full.pdf

Veale, E. L., Buswell, R., Clarke, C. E., & Mathie, A. (2009). Identification of a region in the TASK3 two pore domain potassium channel that is critical for its blockade by methanandamide. *British Journal of Pharmacology*, *152*(5), 778–786. https://doi.org/10.1038/sj.bjp.0707436

Watari, H., Tose, A. J., & Bosma, M. M. (2013). Hyperpolarization of resting membrane potential causes retraction of spontaneous $Ca(i)^{2+}$ transients during mouse embryonic circuit development. *The Journal of Physiology*, *591*(Pt 4), 973–983. https://doi.org/10.1113/jphysiol.2012.244954